HEFAT2003
2nd International Conference on Heat Transfer, Fluid Mechanics and Thermodynamics
23 – 26 June 2003, Victoria Falls, Zambia
Paper number: K4

MICROCHANNEL HEAT TRANSFER, PRESSURE DROP AND MACRO PREDICTION METHODS

M. A. Kedzierski
National Institute of Standards and Technology
Bldg. 226, Rm B114
Gaithersburg, MD 20899,
USA,
E-mail: Mark.Kedzierski@NIST.GOV

ABSTRACT

Advances in the basic understanding of fluid physics have opened an era of unprecedented application of heat transfer processes, and fluid dynamics systems using microchannels. One of the greatest obstacles to the application of leading edge fluid physics science is the lack of engineering tools. For example, is it appropriate to use macro predictive methods for sizing microchannels for desired single-phase heat transfer and pressure drop? Some published data on friction characteristics in microchannels shows a significant disparity between microchannel data and macro-channel predictions. In short, single-phase laminar and turbulent heat transfer and pressure drops in microchannels can differ greatly from macro scale predictions. This manuscript examines several phenomena in terms of potentially causing a difference between "micro" measurements and "macro" prediction methods. Expressions for the tube diameter for which these factors become influential are calculated. Three data sets from the literature were examined to determine if the "micro factors" could have possibly influenced the measurements.

INTRODUCTION

Microtechnologies are improving the speed and reducing the costs of a host of technologies such as DNA analysis and computer chip cooling. One of the greatest obstacles to the design of micro devices is the lack of heat transfer engineering tools. Application of microchannel heat exchange devices requires the ability to predict the single-phase heat transfer and friction in microchannels in the range of 10 μm to 100 μm hydraulic diameter. Currently, existing prediction methods are in question because there is an apparent disparity between the prediction of single-phase heat transfer and pressure drop using macro-flow equations and the measurement of flows and heat transfer in 20 μm to 300 μm channel diameters.

Ameel et al. [1] and others have shown that much of the experimental microchannel heat transfer and pressure drop data from the literature differ significantly from macro prediction methods. Figure 1 shows that both laminar and turbulent single phase heat transfer for microchannels can differ significantly from the macro solutions. Laminar single-phase heat transfer measurements were shown by Ameel et al. [1] to be more than five orders of magnitude less than laminar macro solutions for Reynolds numbers less than 200. In contrast, some turbulent single-phase heat transfer measurements were shown to be more than four orders of magnitude greater than macro predictions for Reynolds numbers larger than 10 000. Figure 2, also taken from Ameel et al. [1], shows that laminar friction factors from the literature are as much as 20 % less than macro theory. While turbulent friction factor measurements vary

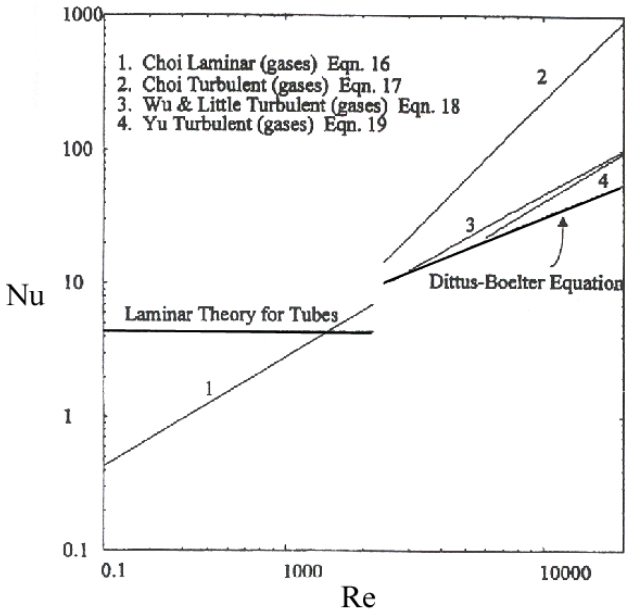

Figure 1: Single-Phase Microchannel Nusselt numbers from Literature [1]

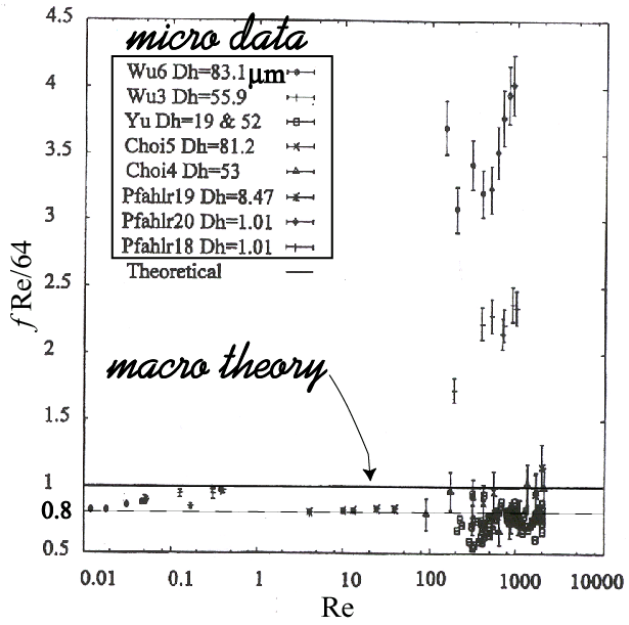

Figure 2: Single-Phase Microchannel Nusselt numbers from Literature [1]

between 50 % less and 300 % greater than that predicted by macro theory.

For the purposes of this manuscript, the "macro-flow" equations for heat transfer and pressure drop are those equations that have been traditionally employed to calculate the single-phase, incompressible Nusselt number (Nu) and Fanning friction factor (*f*). Kays and Crawford [2] provide the following expression for the Fanning friction factor for laminar flow in a round tube:

$$f = \frac{16}{\mathrm{Re}} \tag{1}$$

and give for turbulent flow:

$$f = 0.079\,\mathrm{Re}^{-0.25} \tag{2}$$

Note that the Moody Chart [3] can be used rather than eq. (2) to account for the effect of surface roughness.

Kays and Crawford [2] also give the Nusselt number for laminar flow in a round tube for the constant temperature (Nu_T) and the constant heat flux ($\mathrm{Nu}_{q"}$) boundary condition:

$$\mathrm{Nu}_T = 3.658 \tag{3a}$$

$$\mathrm{Nu}_{q"} = 4.364 \tag{3b}$$

Incropera and DeWitt [4] provide the Dittus-Boelter equation for the turbulent Nu:

$$\mathrm{Nu} = 0.023\,\mathrm{Re}^{0.8}\,\mathrm{Pr}^{n} \tag{4}$$

where $n = 0.4$ for heating and $n = 0.3$ for cooling. Comparable results for turbulent Nussult numbers can be obtained from the more "accurate" but more complicated Petukhov-Popov equation [5].

NOMENCLATURE

a	speed of sound in vapor, m/s
c_p	constant pressure specific heat of the fluid, kJ/kg·K
c_v	constant volume specific heat of the fluid, kJ/kg·K
d	molecular diameter, m
D	tube diameter, m
D_h	hydraulic diameter of channel, m
$D_{1\%}$	diameter for 1 % effect, m
f	Fanning friction factor
G	mass velocity, kg/m^2·s
h	heat transfer coefficient, W/m^2·K
H	characteristic channel dimension, m
j_h	Colburn *j* factor
k	thermal conductivity, W/m·K
k_b	Boltzmann's constant, 1.381×10^{-26} kJ/K
l	mean free path of molecule, m
Kn	Knudsen number, eq. (5)
M	mass, kg
Ma	Mach number $\frac{\bar{u}}{a}$
$\dot{m}$	mass flow rate, kg/s
n	exponent constant in eq. (4)
Nu	Nusselt number $\frac{hD_h}{k}$
P	pressure, N/m^2
Pr	Prandtl number $\frac{c_p\mu}{k}$
q_c	convection duty, W
q_v	viscous dissipation energy, W
$q_c"$	convective heat flux, W/m^2
$q"$	average wall heat flux, W/m^2
R	ideal gas constant, kJ/kg·K
Re	Reynolds number $\frac{\bar{u}D_h}{\nu}$
T	temperature, K
T_w	temperature at wall, K
u	velocity in axial (*x*-)direction, m/s
u_w	*u*-velocity at wall (slip velocity), m/s
u'	turbulent fluctuating *u*-velocity, m/s
x	direction coordinate along channel axis, m
y	direction coordinate normal to the surface, m

Greek symbols

α	molecular thermal diffusivity, m^2/s
γ	c_p/c_v

ΔL channel length, m
ΔP pressure drop across ΔL, kg/m·s^2
ε_H eddy diffusivity for heat transfer, m^2/s
ε_M eddy diffusivity for momentum, m^2/s
η Kolmogorov length scale, m
κ eddy wave number
λ Taylor length scale, m
μ dynamic viscosity, kg/m·s
ν kinematic viscosity, m^2/s
ρ mass density of liquid, kg/m^3
σ liquid-vapor surface tension, kg/s^2
τ_w wall shear stress, kg/ m·s^2

Subscripts
b bulk
c convection
l liquid
q" constant wall heat flux
T constant wall temperature
v vapor
vw vapor at wall
w wall
ϕ viscous dissipation

Superscripts
- average

PLAUSIBLE MICRO INFLUENCES

Various momentum and energy effects for flow and heat transfer that are typically neglected for macroflows become increasingly important as the channel diameter decreases to the microscale. Much of the discrepancy between macro predictions and micro measurements may be resolved by considering the impacts of viscous dissipation [6], thermally developing flow, mixed isothermal and isoflux boundary conditions, and other phenomenon as applied to microchannels [7]. Other influences such as velocity slip, temperature jump, surface roughness, flow maldistribution, micro turbulent effects, electric double layer, composite manufacturing, and size dependent viscosity play roles in microfluidics. Each effect becomes important for different channel sizes. The lack of consideration of these effects may in part be the cause of the apparent discrepancy between macro predictions and micro measurements.

Velocity Slip

The size of the channel relative to the mean free path of the molecule determines the form of the momentum equation that can be used to model the flow. Predictive complications arise when channel diameters approach the scale of the mean free path of the molecule. For example, slip flow must be considered when the tube diameter approaches the mean free path of the molecule. The Knudsen number (Kn) is the ratio of the mean free path of the molecule (l) to the characteristic channel dimension (H):

$$\mathrm{Kn}=\frac{l}{\mathrm{H}} \tag{5}$$

The Kn is essential for determining how to model the flow.

The Kn for an ideal gas in a tube of diameter D can be expressed as [8]:

$$\mathrm{Kn}=\frac{k_b T}{\sqrt{2}\pi d^2 PD} \tag{6}$$

where k_b is the Boltzmann constant, d is the molecular diameter, P is the pressure, and T is the temperature of the gas.

Table 1 provides tube diameters that correspond to different Kn flow regimes: continuum flow, continuum with slip flow, slip flow, and free molecule flow. The Kn is used to define the boundary of each flow regime. Continuum flow, where the velocity profile is continuous everywhere and is zero at the wall, is observed for Kn < 0.001. Here, the "macro-flow" Navier-Stokes equations are valid. For the fluids given in Table 1, vapor flow in tubes with diameters larger than 200 μm may be modeled by the Navier-Stokes equations. The remaining flow regimes are rarefied. Rarefied flow, or flow with a non-continuous velocity distribution, results when the frequency of interaction between the molecules of the fluid and the wall is reduced. Information regarding the existence of the wall is transferred infrequently between molecules when the characteristic length of the channel approaches l. As a result, a non-zero velocity at the wall or a *slip velocity* (u_w) occurs from the lack of local equilibrium between the wall and the fluid. The slip flow regime exists for 0.001 < Kn < 0.1 [9] where the flow may be modeled by the Navier-Stokes equations with a slip boundary condition [8]. As shown in Table 1, gas flow in tubes with diameters between 200 μm and approximately 0.5 μm fall within the continuum/slip flow regime and require consideration of the slip boundary condition. For 0.1 < Kn < 3, full slip flow, the Navier-Stokes equations are no longer valid [8]. The Boltzmann equation, which is based on a single-particle velocity distribution, may be used to model flow for 0.1 < Kn < 3 [10]. Here the molecules are stochastically modeled via the single-particle velocity distribution. Tube

Table 1 Tube Diameters for Different Flow Regimes

Gas	molecular mean free path (A)	D for Kn = 0.001 (μm)	D for Kn = 0.1 (μm)	D for Kn = 3 (μm)
He	1860	186	1.86	0.06
Ne	1320	132	1.32	0.04
Ar	666	66.6	0.67	0.02
H_2	1180	118	1.18	0.04
N_2	628	62.8	0.63	0.02
O_2	679	67.9	0.68	0.02
CO_2	419	41.9	0.42	0.01
NH_3	451	45.1	0.45	0.01
CH_4	516	51.6	0.52	0.02
air	700	70.0	0.70	0.02

diameters between approximately 2 μm and 0.01 μm fall within this regime for gases. For Kn > 3, free molecule flow exists where the body has no influence on the velocity distribution [9]. Table 1 shows that free molecule gas flow may occur at a diameter of 0.06 μm.

Maxwell [11] derived an expression for the slip velocity at the wall for a gas based on the velocity (u) gradient normal to the wall:

$$u_w \approx l\left(\frac{du}{dy}\right)_w \tag{7}$$

Using the definition of the shear stress (τ_w) and the Reynolds number (Re), Maxwell's slip velocity can be expressed in terms of the Fanning friction factor (f) as:

$$\frac{u_w}{\bar{u}} = l\frac{\rho\bar{u}}{\mu}\frac{f}{2} = l\frac{\mathrm{Re}}{D}\frac{f}{2} \tag{8}$$

where $\bar{u}$ is the average fluid velocity and μ and ρ are the dynamic viscosity and the density of the fluid, respectively.

Substituting Maxwell's approximation for the mean free path length for nonpolar dilute gases into the above expression and, in addition, the turbulent and the laminar friction factors (eqs. (1) and (2)) yields for turbulent vapor flow:

$$\frac{u_w}{\bar{u}} = 0.0334\frac{\mu_v\,\mathrm{Re}_v^{0.75}}{a\rho_v D} \tag{9}$$

and for laminar vapor flow:

$$\frac{u_w}{\bar{u}} = \frac{12\mu_v}{a\rho_v D} \tag{10}$$

where a is the speed of sound in the vapor.

Similar expressions may be obtained for liquid flows by approximating the mean free path of a liquid to be 1 Angstrom. The slip velocity ratio for turbulent liquid flow becomes:

$$\frac{u_w}{\bar{u}} = \left(0.039\times10^{-10}\,\mathrm{m}\right)\frac{\mathrm{Re}^{0.75}}{D} \tag{11}$$

and that for laminar liquid flow is:

$$\frac{u_w}{\bar{u}} = \frac{8\times10^{-10}\,\mathrm{m}}{D} \tag{12}$$

Equations 11 and 12 were rearranged and solved for the tube diameter where u_w is 1 % of the average fluid velocity ($D_{1\%}$).

Figure 3 plots $D_{1\%}$ versus Reynolds number for turbulent and laminar flow. In general, Fig. 3 shows that the slip velocity is negligible for tube diameters larger than 50 μm for laminar air flow. The $D_{1\%}$ diameters for turbulent air flow are more than double that for laminar flow and they are a function of Reynolds numbers: 100 μm to 250 μm for Re from 6000 to 20000. The $D_{1\%}$ diameters for water flow are approximately two orders of magnitude smaller than the air flow diameters. For example, the $D_{1\%}$ for laminar water is 0.08 μm, while turbulent water $D_{1\%}$ varies between 0.23 μm and 0.66 μm for a Re variation between 6000 and 20000.

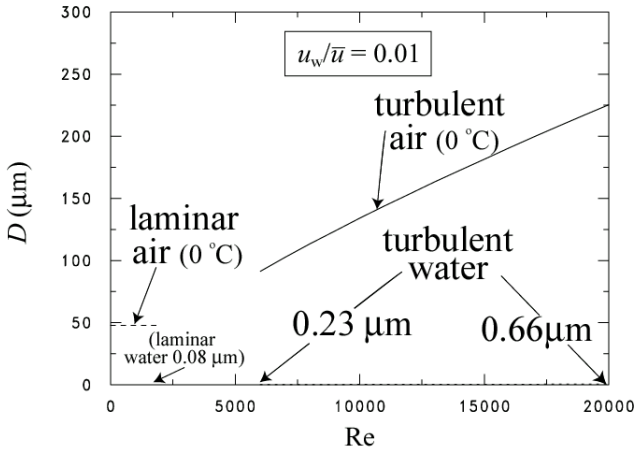

Figure 3: Tube Diameter Where Slip Velocity is 1 % of the Average Fluid Velocity

Temperature Jump

Another consequence of infrequent communication of molecules with the wall due to the characteristic length approaching the mean free path is a *temperature jump* at the wall. Here the molecules are less able to be in local equilibrium with the wall because of reduced energy exchange with it. As a result, the vapor temperature at the wall (T_{vw}) and the wall temperature (T_w) differ by the temperature jump (T_{vw} - T_w). For tubes, White [12] expresses this difference as:

$$\frac{T_{vw}-T_w}{T_b-T_w} = 0.87\frac{\mu_v\,\mathrm{Re}_v\,f_v}{a\rho_v D} \tag{13}$$

where T_b is the temperature of the bulk fluid.

Substituting the Fanning friction factor for turbulent flow (eq. (2)) into eq. (13) yields an expression for temperature jump for a turbulent vapor:

$$\frac{T_{vw}-T_w}{T_b-T_w} = 0.068\frac{\mu_v\,\mathrm{Re}_v^{0.75}}{a\rho_v D} \tag{14}$$

A similar procedure using eqs. (13) and (1) yields the temperature jump for a laminar vapor:

$$\frac{T_{vw} - T_w}{T_b - T_w} = \frac{13.92\mu_v}{a\rho_v D} \tag{15}$$

Equations 14 and 15 were used in Fig. 4 to plot the tube diameter where the temperature jump is 1 % of the driving temperature difference (T_b - T_w). As Fig. 4 shows, tubes with diameters larger than 56 μm exhibit negligible temperature jump for laminar air flow. Turbulent flow diameters for 1 % temperature jump are marginally larger and a function of Reynolds number being approximately 200 μm and 450 μm at Reynolds numbers of 6000 and 20000, respectively.

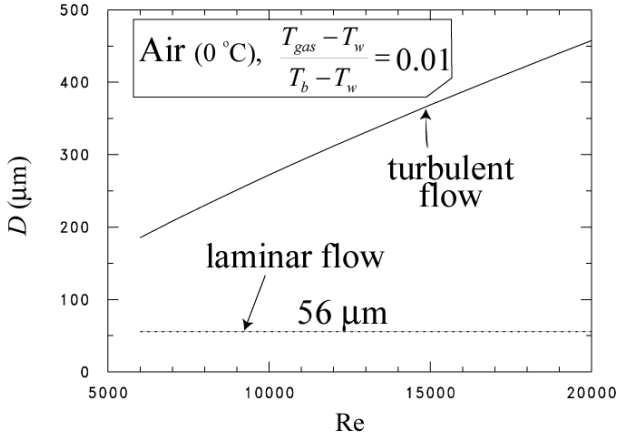

Figure 4: Tube Diameter Where Temperature Jump is 1 % of Driving Temperature Difference

Figure 5 shows the effect of temperature jump on the liquid heat transfer as calculated by Tunc et al. [13] for a constant wall temperature. Figure 5 compares the fully developed Nusselt number (Nu) accounting for the temperature jump to that with no temperature jump. The figure shows that for Kn = 0.02, the Nu with temperature jump is approximately 15 % greater than the Nu without temperature jump. For water, a Kn of 0.02 is approximately equivalent to a tube diameter of 0.005 μm. At a Kn of 0.09 ($D \cong$ 0.001 μm), the Nu with a temperature jump is more than 70 % larger than the Nu without considering the temperature jump.

Viscous Dissipation

For fixed fluid properties, high fluid velocities are more readily attained for a given Reynolds number in microchannels than for macrochannels. For this reason, frictional heating due to viscous dissipation is more of a factor for a given Re for microchannels than it is for macrochannels. Consequently, care must be taken in reporting measurements and calculating predictions for comparison to measurements to ensure that the effects of viscous dissipation are included. For example, if viscous dissipation is significant, then the temperature rise of a fluid caused by it must be accounted for in the first law analysis when calculating the heat duty of a microchannels. The measured temperature change cannot be the only input in calculating the duty of the test section for small diameter test

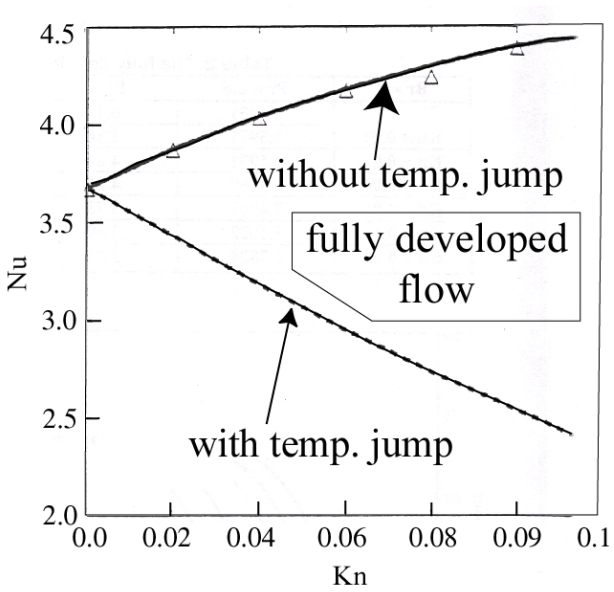

Figure 5: Fully Developed Nu With and Without Temperature Jump at Wall for Liquid [13]

sections when viscous dissipation is important. Otherwise, the heat duty will be either underestimated or overestimated depending on whether the test section is heated or cooled. For measurements of cooling fluids, the heat that crosses the control volume will be underestimated if viscous dissipation is not accounted for in the energy balance. As a result, the laminar cooling Nu will decrease with respect to Re rather than being constant. Similarly, the heat duty of heating measurements will be overestimated and increase with Re if viscous dissipation is not accounted for in the energy balance.

Likewise, frictional heating may also alter the driving temperature difference for heat transfer in microchannels. Accounting for viscous dissipation in the calculation of the driving temperature difference requires the use of the adiabatic wall temperature (T_{aw}) rather than the bulk fluid temperature (T_b) to define the temperature difference between the fluid and the wall [14].

Viscous dissipation energy (q_v) can be represented as the frictional part of flow work. If the gradient of the specific volume with respect to the fluid temperature at constant pressure is neglected, the q_v can be estimated in terms of the friction factor for incompressible flow as:

$$q_v = \frac{\dot{m}\Delta P}{\rho} = \frac{2\dot{m}f\Delta L G^2}{\rho^2 D} = \frac{\mu^3 \pi \,\mathrm{Re}^3\, \Delta L}{2D^2\rho^2} f \tag{16}$$

where ΔL is the length of the channel.

Equation (16) can be normalized by convection ($q_c = q_c'' \pi D \Delta L$) to obtain the relative contribution of viscous dissipation and convection:

$$\frac{q_v}{q_c} = \frac{\mu^3 \mathrm{Re}^3}{2q_c^{"} D^3 \rho^2} f \tag{17}$$

Substitution of eq. (2) into this expression gives the ratio of viscous dissipation to convection for turbulent flow:

$$\frac{q_v}{q_c} = \frac{0.039\mu^3 \mathrm{Re}^{2.75}}{\rho^2 D^3 q_c^{"}} \tag{18}$$

Likewise, eq. (1) can be substituted into eq. (17) to obtain the ratio of viscous dissipation to convection for laminar flow:

$$\frac{q_v}{q_c} = \frac{8\mu^3 \mathrm{Re}^2}{\rho^2 D^3 q_c^{"}} \tag{19}$$

Equation (19) can also be obtained by using the Suryanarayana [15] definition of the axial temperature gradient due to viscous dissipation $\left(\frac{\partial T_b}{\partial x}\right)_\phi$ for a laminar, incompressible fluid:

$$\left.\frac{\partial T_b}{\partial x}\right|_\phi = 2\frac{\mu}{\rho c_p u}\left(\frac{\partial u}{\partial r}\right)^2 \cong 32\,\mathrm{Re}\frac{\nu^2}{c_p D^3} \tag{20}$$

Using eq. (20), the ratio of viscous dissipation energy flux ($q_v^{"}$) to the convective energy flux without viscous dissipation ($q_c^{"} = \frac{\dot{m} c_p}{\pi D}\frac{\partial T_b}{\partial x}$) can be estimated for laminar flow in a circular tube as:

$$\frac{q_v^{"}}{q_c^{"}} = \frac{q_v}{q_c} = \frac{\left.\frac{\partial T_b}{\partial x}\right|_\phi}{\left.\frac{\partial T_b}{\partial x}\right|_c} = 8\,\mathrm{Re}^2\frac{\nu^3\rho}{q_c^{"} D^3} \tag{21}$$

which is the same expression as given in eq. (19).

Equations 18 and 19 are used to illustrate the tube diameter where q_v is 1 % of the convective heat transfer ($D_{1\%}$). Here, vapor flow is considered to be incompressible if the Mach Number is less than 0.3, $\mathrm{Ma} = \frac{\mu\,\mathrm{Re}}{a\rho D} \le 0.3$, [16]. Figure 6 illustrates the effect of viscous dissipation on laminar and turbulent liquid and vapor flow for two heat fluxes (1 kW/m^2 and 50 kW/m^2), and shows that viscous dissipation heating can be significant. This is especially true for turbulent vapor flow and smaller heat fluxes: $D_{1\%}$ is approximately 20 mm for air at 273 K and Re = 20 000. Laminar liquid at the higher heat flux is the least affected by viscous dissipation: $D_{1\%}$ = 0.38 mm for water at 300 K and Re = 2300.

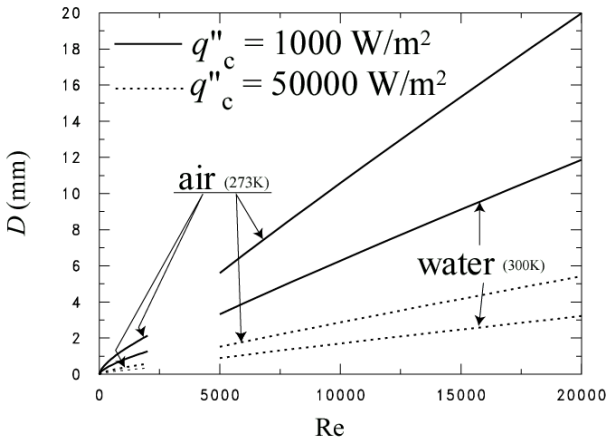

Figure 6: Diameter Where Viscous Dissipation Energy is 1 % of Convection

Developing Flow

Yu et al. [7] caution that the entry length should be calculated considering that microfluidic devices may have a small length to diameter ratio. Expressions given by Kays [17] and Whitaker [18] can be used to estimate the entry length for laminar and turbulent flow. In general, fully developed laminar flow can be expected for $\frac{x/D}{\mathrm{Re}\,\mathrm{Pr}} > 0.05$, while fully developed turbulent flow is achieved for $x/D \cong 30$ for Pr = 0.7 (vapor) and $x/D \cong 20$ for Pr = 10 (liquid). However, the turbulent entry length is a strong function of Pr.

Turbulent Flow and Eddy Bursting

Turbulent single-phase flow continuum is satisfied if the size of the smallest turbulent eddies ($\eta = 2\pi/\kappa$) is much larger than the mean free path of the molecules (l). Approximations for the eddy wave number (κ) indicate that continuum for turbulence will exist for a liquid if $\eta \gg 4\,\text{Å}$ and for a vapor if $\eta \gg 1000\,\text{Å}$. The smallest eddies become smaller as the channel cross section is decreased. If the size of the smallest eddies approach the mean free path of the molecule, then continuum is not satisfied. Not much experience in turbulent modeling is available for no continuum.

Even when continuum exists there can be differences between micro and macro turbulent flow and heat transfer. For example, Yu et al. [19] have used *turbulent eddy bursting phenomenon* [2] to explain differences between micro measurements (Kn < 0.001) and macro predictions for turbulent single phase heat transfer and incompressible flow. Kays and Crawford [2] point out that eddy bursting occurs infrequently for macro turbulent flow. The difference for micro flow is that the frequency of the bursting event increases significantly. The Yu et al. [19] hypothesis is based on Taylor length scales. In traditional turbulent, macro heat transfer, the energy associated

with the Taylor length scale is delivered to the viscous sublayer via the fluctuating velocity component *u'*. But because the Taylor length scale (λ) is of the same order of magnitude of the tube diameter, *u'* does not vanish at the viscous sublayer, rather, it bypasses the wall layer and transfers directly to the wall. Consequently, there is an additional heat transfer to the wall mechanism for microchannels ($u'(T_w - T_b)$) as compared to macro turbulent flow that contributes to the total heat flux as:

$$\frac{q''}{\rho c_p} = (\alpha + \varepsilon_H)\frac{dT}{dy} + u'(T_w - T_b) \qquad (22)$$

where *y* is the direction coordinate normal to the surface, α is the molecular thermal diffusivity, and ε_H is the eddy diffusivity for heat transfer.

Similarly, there is an additional momentum transfer mechanism ($\overline{u'u'}$) as compared to macro turbulent flow. Yu et al. [19] claim that the additional momentum transfer mechanism causes the pressure drop in microchannels to be less than that as compared to macro turbulent flow. The Yu et al. [19] expression for turbulent shear stress (τ) for microchannels and Kn < 0.001 is:

$$\frac{\tau}{\rho} = (\nu + \varepsilon_M)\frac{du}{dy} + \overline{u'u'} \qquad (23)$$

where ε_M is the eddy diffusivity for momentum, and $\overline{u'u'}$ is the Reynolds stress.

Yu et al. [19] provide the Colburn j factor (j_h) for the eddy bursting effect:

$$j_h = \frac{f}{2}\left(1 + \frac{\mathrm{Re}\,\lambda / D}{1 + \varepsilon_M / \nu}\right) \qquad (24)$$

which reduces to the macro equation for $\frac{\mathrm{Re}\,\lambda / D}{1 + \varepsilon_M / \nu} = 0$.

Consequently, the $\frac{\mathrm{Re}\,\lambda / D}{1 + \varepsilon_M / \nu}$ can be used as a measure of the effect of the eddy bursting effect. Figure 7 illustrates the diameter of the tube when the eddy bursting effect enhances the microchannel heat transfer by 10 %. The Taylor length scale was estimated to be 3 mm, while the ε_M/ν ratio was calculated from simple Prandtl mixing length theory. For Reynolds numbers between 5000 and 20000, the eddy bursting effect does not have 10 % or more effect until the diameters are smaller than approximately 2 μm or less.

On the other hand, the increased eddy-bursting hypothesis for microchannel has at least one detractor. Kakac et al. [20] conjecture that the fluid flow and heat transfer turbulent eddy mechanism may in fact be suppressed for tube diameters less than 2 mm. The state of turbulence modeling in turbulent flow

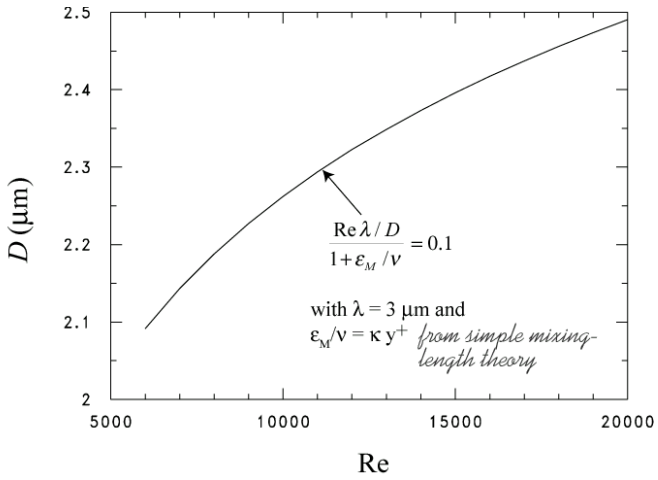

Figure 7: Diameter Where Eddy Bursting Causes a Heat Transfer Enhancement of 10 %

is best summed up by Ghiaasiaan and Abdel-Khalik [21]: …*the lack of adequate understanding of turbulence in microchannels is believed to be the main reason for disagreement between existing data and commonly used correlations for large channels.*

Size Dependent Viscosity

Xu et al. [22] discuss how the viscosity of polar and non-polar fluids are affected by channel size. The balance between the molecular repulsive force and the attractive force is affected by the confined space. The attractive forces between polar molecules are greater than those between non-polar molecules. Figure 8 shows that the viscosity of water in a 0.01 μm diameter channel is 10 % less than water in macrochannels.

Roughness

Microchannel laminar flow is consistent with macro flow in that surface roughness has little or no effect on the magnitude of the pressure drop with the exception of possibly early transition to turbulence [23]. The Moody chart may predict the influence of roughness on turbulent flow in microchannels; however, there are relatively large uncertainties associated with surface roughness measurements in microchannels [24]. Consequently, there may be errors in the prediction of the effect of roughness due to the uncertainty in the microchannel roughness.

Flow Mal-Distribution

Rao and Webb [25] have investigated the effects of flow mal-distribution in microchannels. They conclude that mal-distributed flow between multi-parallel passages in microchannel test sections may be the major cause for the apparent discrepancy between microchannel measurements and macro predictions. The mal-distribution is caused by differences in the size of adjacent channels. The conclusion is supported by noting that single microchannel heat transfer and

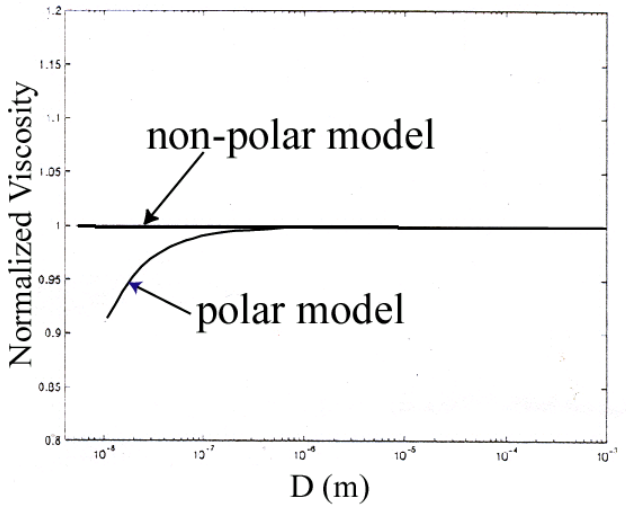

Figure 8: Effect of Channel Size on Viscosity [21]

friction measurements are typically within 20 % of macro-scale flows.

Compressible Flow

When vapor flows at a high velocity (Ma > 0.3) its density is likely to vary significantly with respect to the flow direction [16]. If this occurs, the flow is said to be compressible. The change in density along the flow length induces a change in velocity in the axial direction for fixed mass flow and channel cross section. The axial velocity gradient is neglected for incompressible flows and for the macro relations given in eqs. (1-4). Consequently, there are additional velocity terms in the momentum and energy equations that are required to model compressible flows. The flow begins to become compressible for Mach numbers greater than 0.3. Generally, liquids are not compressible unless exposed to very large pressures. Consequently, an expression for tube diameter to ensure that Ma > 0.3 can be expressed in terms of the Re for an ideal gas as:

$$D \geq \frac{\mu \,\mathrm{Re}}{0.3\rho\sqrt{\gamma \mathrm{R}T}} \tag{25}$$

where $\sqrt{\gamma \mathrm{R}T}$ is the ideal gas expression for the speed of sound [26] with $\gamma = c_p / c_v$ and R as the ideal gas constant.

DISCUSSION

This section examines the experimental measurements of Wu and Little [27] and Choi et al. [28] to determine which of the plausible "micro factors" listed above may be affecting the measurements.

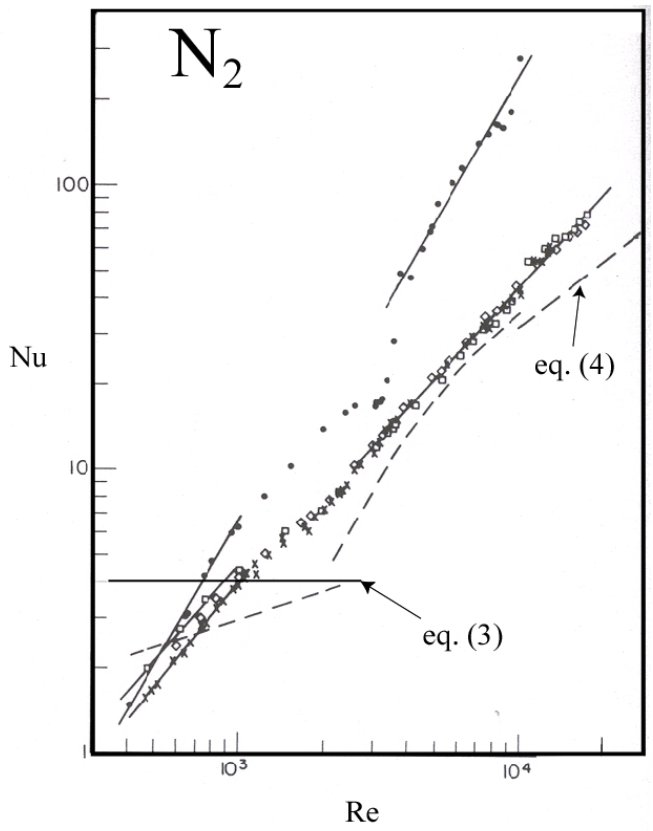

Figure 9: Wu and Little [27] Nu versus Re measurements for microchannels

Laminar Vapor

Figure 9 shows the laminar Nusselt numbers for nitrogen taken by Wu and Little [27] in a composite channel. The channel was constructed from a rough groove and a smooth top giving a trapezoidal cross section and a hydraulic diameter of 155 μm. Most of the Wu and Little [27] measurements for Re < 700 are shown to be less than the macro laminar solution (≈ 4). Similarly, measurements for Re > 700 are shown to be greater than the macro laminar solution. Also note that the measured Nu is not a constant, but increases with Reynolds number.

Several of the micro factors appear not to pertain to the Wu and Little [27] laminar data set. For example, the Kn calculated from eq. (5), while substituting D_h (155 μm) for H and obtaining the mean free path of N_2 from Table 1, is 0.0004, indicating that continuum exists and that the Navier-Stokes equations are valid for this data set. The slip ratio from eq. (10) confirms that the slip velocity is negligible ($u_w / \overline{u} = 0.003$). Likewise, eq. (15) illustrates that the temperature jump is only approximately 0.3 % of the driving temperature difference. Because it is laminar flow, the roughness should have little effect. The channel diameter is much larger than 0.01 mm. So the liquid viscosity should not be affected by the size of the channel. In addition, the channel is single channel flow, as a result, flow maldistribution cannot affect the measurements.

Developing flow is probably not a factor because the L/D = 200 and developing flow would cause the Nu to be greater than the fully developed solution (≈ 4). Figure 9 shows that most of the laminar Nusselt numbers are less than 4.

The two factors that appear to be significant for the Wu and Little [27] laminar data set are viscous dissipation and compressible flow. The compressible flow regime begins at approximately Re = 1100 for D_h = 155 μm. Consequently, compressible flow does not affect most of the laminar measurements. Conversely, viscous dissipation effects appear to be significant for most of the data. For example, the energy balance used by Wu and Little [27] did not account for viscous dissipation. The temperature rise due to viscous dissipation for Ma < 0.3, estimated from eq. (16), was 20 K and 58 K at Re of 400, and 1162, respectively. Although, viscous dissipation appears to be significant for this data set, it is not clear that the viscous dissipation is responsible for the deviation of the measured Nu from the macro solution. Although it cannot be confirmed in the Wu and Little [27] manuscript, both cooling and heating data appear to have been taken. If this were the case, and if viscous dissipation were the sole cause of the discrepancy due to its neglect in the energy balance, then the cooling Nu would have a negative slope with respect to the Re, while the heating Nu would have a positive slope with respect to Re. The Wu and Little [27] laminar Nu only exhibit a positive slope with respect to Re. Thus, is not clear that viscous dissipation is the sole cause of the deviation of the measured Nu from the macro solution for Nu.

Figure 10 shows the laminar Nusselt numbers for nitrogen taken by Choi et al. [28] in a circular channel. The channel roughness-to-diameter ratio varied between 0.001 and 0.0002 with an inside diameter of 9.7 μm. Nearly all the laminar measurements are less than the laminar macro solution. The Wu and Little [27] laminar measurements are between 50 % and 100 % greater than the Choi et al. [28] measurements. The Choi et al. [28] Nu have a similar slope with respect to the Re.

Fewer of the micro factors appear not to pertain to the Choi et al. [28] laminar data set as compared to the Wu and Little [27] laminar data set. The roughness should have little effect because the flow is laminar and the roughness ratio is relatively small. The channel diameter is much larger than 0.01 mm. Consequently, the liquid viscosity should not be affected by the size of the channel. In addition, flow maldistribution cannot affect the measurements because it is a single channel. Developing flow is probably not a factor because L/D is between 640 and 8100 and, as for the Wu and Little [27] measurements, developing flow would cause the Nu to be greater than the fully developed solution (~4).

There are several micro effects that do appear to be significant for the Choi et al. [28] laminar data set. For example, the Kn (D = 9.7 μm) calculated from eq. (5), (0.006) indicates that slip flow exists. Hence, a slip boundary condition is necessary in order to solve the Navier-Stokes equations for this data set. The slip ratio from eq. (10) confirms that the slip velocity is not negligible ($u_w / \overline{u} = 0.05$). Likewise, eq. (15)

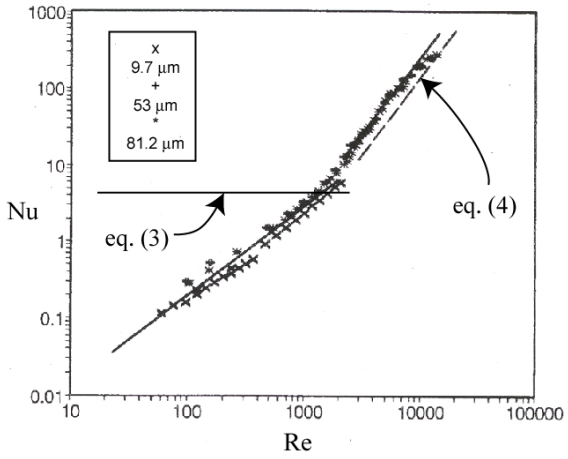

Figure 10: Choi et al. [28] Nu versus Re measurements for microchannels

illustrates that the temperature jump is approximately 5 % of the driving temperature difference. The energy balanced used by Choi et al. [28] did not account for viscous dissipation. The temperature rise due to viscous dissipation for Ma < 0.3, estimated from eq. (16), was 2940 K and 10 584 K at Re of 20, and 72, respectively. The estimate from eq. (16) is obviously in error probably because it is not valid for slip flow. Compressible flow exists for Re greater than approximately 70 for this data set.

Turbulent Vapor

Figure 10 shows the turbulent Nusselt numbers for nitrogen taken by Choi et al. [28] in a circular channel. The channel roughness-to-diameter ratio was 0.0002 with an inside diameter of 81.2 μm. Nearly all the turbulent measurements are approximately 100 % greater than the turbulent macro solution. Some of the Choi et al. [28] turbulent Nu are as much as 200 % greater than those of the Wu and Little [27] measurements for the same Re. In addition, the general slope of the Nu versus Re data differ significantly for the two data sets.

The Kn for the turbulent Choi et al (1991) data is 0.0007, indicating that the Navier-Stokes equations are valid. However, eq. (9) reveals that slip flow exists (0.01 to 0.02) for the larger Re. Likewise, the temperature jump as calculated with eq. (14) is 2 % to 5 % of the driving temperature difference. Considering that the data are turbulent, the roughness should affect the results. The eddy bursting term, $\frac{\mathrm{Re}\,\lambda / D}{1+\varepsilon_M / \nu}$, was found to be negligible. The entry length should not be a factor considering that L/D ranged between 640 to 8100, which is significantly larger than 30. The viscous dissipation effect could not be calculated because eq. (18) was out of range for Re > 608 (Ma = 0.3). The data become compressible at Re of approximately 550. This may be the

main reason for the difference between the traditional macro heat transfer given in eq. (4) and the turbulent measurements. Nevertheless, slip, temperature jump, roughness, and viscous dissipation all contribute to the apparent difference between the Choi et al. [28] turbulent vapor heat transfer measurements and macro predictions.

CONCLUSIONS

The apparent disparity between the prediction of single-phase heat transfer and pressure drop using macro-flow equations and the measurement of flows in 20 μm to 300 μm channel diameters may be due to many simultaneous factors. Some of these factors may be new phenomenon associated with microchannels such as enhanced eddy bursting and early transition to turbulence. Others may be known phenomena that are typically neglected for macro flow and heat transfer such as slip flow, viscous dissipation, and compressible flow. Expressions were derived to illustrate the tubes diameter where each factor becomes influential. Of all the factors, viscous dissipation was shown to be the largest contributor to the difference between microchannel measurements and traditional macro predictions. Viscous dissipation was shown to be influential for tubes of millimeters in diameter, while most other effects were important for tube diameters of tenth of millimeters or microns. Compressible flow was shown to be prevalent, but it was not quantified. Slip flow and temperature jump were evident for the measurements from the literature that were examined. The effects of flow mal-distribution in microchannels could not be demonstrated. The eddy bursting effect was not realized for tubes larger than 2 μm. The potential for disparity between micro and macro heat transfer and flow is greater for vapor than it is liquids. The "micro effects" occur for larger tube diameters for vapors than for liquids.

The apparent difference between micro and macro heat transfer could largely be due to microchannel data reduction methods not accounting for viscous dissipation in the calculation/measure of the global duty of the test section. Considering the possible importance of viscous dissipation, a method for reliably calculating viscous dissipation effects with slip flow is required.

ACKNOWLEDGEMENTS

This work was funded by NIST's Advance Technology Program under project manager Dr. G. Georgevich. Thanks go to the following people for their constructive criticism of the first draft of the manuscript: Mr. D. Yashar, and Dr. D. Didion (retired) of NIST and Dr. J. Kim of the University of Maryland.

REFERENCES

[1] Ameel, T. A., Warrington, R. O., Wegeng, R. S., and Drost, M. K., 1997, "Miniaturization Technologies Applied to Energy Systems," Energy Convers. Mgmt., Vol. 38, No. 10-13, pp. 969-982.

[2] Kays, W. M., and Crawford, M. E., 1980, Convective Heat and Mass Transfer, 2nd Ed., McGraw-Hill, New York, p. 182-183.

[3] White, F. M., 1979, Fluid Mechanics, McGraw-Hill, Inc., New York, p. 333.

[4] Incropera, F. P., and DeWitt, 1981, Fundamentals of Heat Transfer, John Wiley & Sons, New York.

[5] Gnielinski, V., 1976, "New Equations for Heat and Mass Transfer in Turbulent Pipe and Channel Flow," Int. Chem. Engineering, Vol. 16, pp. 359-368.

[6] Webb, R. L, 1998, Private Communications, The Pennsylvania State University.

[7] Yu, S., Ameel, T., and Xin, M., 1999, "An Air-Cooled Microchannel Heat Sink with High Heat Flux and Low Pressure Drop," NHTD99-162, Proceedings of 33rd National Heat Transfer Conference.

[8] Xue, H., and Fan, Q., 2000, "A New Analytic Solution of the Navier-Stokes Equations For Microchannel Flows," Microscale Thermophysical Engineering, Vol. 4, pp. 125-143.

[9] Schaaf, S. A., and Chambre, 1961, Flow of Rarefied Gases, Princeton University Press, NJ.

[10] Martys, N. S., 2001, "A Classical Kinetic Theory Approach to Lattice Boltzmann Simulation," J. Modern Physics C, Vol. 12, No. 8, pp. 1169-1178.

[11] Maxwell, C., 1952, "Scientific Papers of Clerk Maxwell," Vol. 2, Dover, New York.

[12] White, F. M., 1974, Viscous Fluid Flow, McGraw-Hill, Inc., New York, p. 52.

[13] Tunc, G., and Bayazitoglu, Y., 2000, "Heat Transfer for Gaseous Flow in Microtubes with Viscous Heating," Proceedings of the ASME Heat Transfer Division, ASME HTD-Vol. 366-2, pp. 299-306.

[14] McAdams, W. H., 1954, Heat Transmission, McGraw-Hill, 3rd Ed., New York.

[15] Suryanarayana, N. V., 1995, Engineering Heat Transfer, West Pub. Co., St. Paul, pp. 920-921.

[16] White, F. M., 1984, Heat Transfer, Addison-Wesley, Reading, MA, p. 305.

[17] Kays, W. M., 1966, Convective Heat and Mass Transfer, McGraw Hill, New York.

[18] Whitaker, S., 1972, AIChE J., Vol. 18, No. 361.

[19] Yu, D., Warrington, R., Barron, R., and Ameel, T., 1995, "An Experimental and Theoretical Investigation of Fluid Flow and Heat Transfer in Microtubes," Proceedings of ASME/JSME Thermal Engineering Conference, Vol. 1, pp. 523-530.

[20] Kakac, S., Shah, R. K., and Aung, W., 1987, Handbook of Single-Phase Convective Heat Transfer, Wiley, New York.

[21] Ghiaasiaan, S. M., and Abdel-Khalik, S. I., 2001, "Two-Phase Flow in Microchannels", Advances in Heat Transfer, Academic Press, Vol. 34, pp. 145- 254.

[22] Xu, B., Ooi, K. T., Wong, T. N., and Liu, C. Y., 1999, "Study on the Viscosity of the Liquid Flowing in

Microgravity," J. Micromech. Microeng., Vol. 9, pp. 377-384.
[23] Peng, X. F., Peterson, G. P., and Wang, B. X., 1994, "Friction Flow Characteristics of Water Flowing Through Microchannels," Experimental Heat Transfer, Vol. 7, No. 4, pp. 256-283.
[24] Wu, P., and Little, W. A., 1983, "Measurement of Friction Factors for the Flow of Gases in Very Fine Channels Used for Microminiature Joule-Thomson Refrigerators," Cryogenics, No. 5, pp. 273-277..
[25] Rao, P., and Webb, R. L., 2000, "Effects of Flow Mal-Distribution in Parallel Micro-Channels," Proceedings of 34th National Heat Transfer Conference, ASME NHTC-2000 12102.
[26] John, J. E. A., 1984, Gas Dynamics, 2nd ed., Allyn and Bacon, Boston, p. 31
[27] Wu, P., and Little, W. A., 1984, "Measurement of the Heat Transfer Characteristics of Gas Flow in Fine Channel Heat Exchangers Used for Microminiature Joule-Thomson Refrigerators," Cryogenics, No. 5, pp. 415-420.
[28] Choi, S. B., Barron, R. F., and Warrington, R. O., 1991, "Fluid Flow and Heat Transfer in Microtubes," Micromechanical Sensors, Actuators, and Systems, ASME DSC-Vol. 32, pp. 123-134.